LBL-11405
CONF-800765--3

Lawrence Berkeley Laboratory
UNIVERSITY OF CALIFORNIA

Materials & Molecular Research Division

Presented at the 7th LBL/MMRD International Materials Symposium on "Surfaces and Interfaces in Ceramic and Ceramic-Metal Systems", Lawrence Berkeley Laboratory, Berkeley, CA, July 28-August 1, 1980

AN ELECTRON MICROSCOPY ANALYSIS OF A SIMPLE METAL/CERAMIC INTERFACE

U. Dahmen, K.H. Westmacott and G. Thomas

September 1980

Prepared for the U.S. Department of Energy under Contract W-7405-ENG-48

An Electron Microscopy Analysis of a Simple Metal/Ceramic Interface

U. Dahmen, K. H. Westmacott and G. Thomas

Materials and Molecular Research Division,
University of California,
Lawrence Berkeley Laboratory
Berkeley, CA 94720

INTRODUCTION

The study of metal-ceramic interfaces is of fundamental importance in materials science because of the many technological applications for devices fabricated with both metal and ceramic components. For example, MOS devices, metal-ceramic seals, refractory metal alloy coatings to cit only a few. Notwithstanding its importance, the direct study of interfacial structure of metal-ceramic composites by transmission electron microscopy is difficult due to specimen preparation problems. However, some insights into the structures may be obtained through the more indirect but conventional path of forming the ceramic phase in a metal matrix by a precipitation reaction. In the present study high purity tantalum-carbon alloys were prepared and quenched in ultra-high vacuum and aged to produce large precipitates of the stable Ta_2C carbide phase. In addition to determining the orientation relationship, diffraction contrast analysis and lattice fringe imaging techniques were employed to characterize the interface structures.

EXPERIMENTAL PROCEDURES

The material was prepared from 99.9 wt.% pure tantalum by electron beam zone refining. After three passes the single crystal rod of 8mm diameter was rolled into a sheet of 150μm thickness. Small strips were cut from this sheet and carburized to a concentration of about 0.5 at.% at

2000°C first by coating with graphite and later by reaction with acetylene gas. Samples 25 x 3 x 0.15 mm were outgassed and homogenized in ultrahigh vacuum ($\sim 10^{-8}$ torr) by joule heating with ac current prior to either a slow cooling or quenching treatment. The samples were subsequently aged without breaking the vacuum. Discs of 3mm diameter were cut from the center of each sample and thinned for electron microscopy in a double jet polisher using an electrolyte of 4 vol.% H_2SO_4 in methanol at $-30 \pm 5^{\circ}C$ and a current density of $1 Acm^{-2}$. The electron microscopy was done on a 125kV Siemens 102 microscope equipped with a high-tilt/high-resolution goniometer stage.

EXPERIMENTAL RESULTS

(a) Orientation Relationship

All the metal-ceramic interfaces considered in the present study had the same relative orientation of the two crystal lattices, the only variable being the plane of the interface itself. The orientation relationship was constant because the carbide was first nucleated as a coherent precipitate. During the loss of coherency, the orientation relationship remained unaltered even though the particle shape changed. This orientation relationship was determined accurately by examining several low-index sections of reciprocal space as shown in Fig. 1(a). Note in particular that the (110) BCC section was almost, but not completely, parallel to the (0001) HCP section. The hexagonal spot pattern of the carbide outlined in the (110)/(0001) section exhibits a $\sim 5^{\circ}$ rotation from its symmetrical position which brings the $1\bar{1}00$ spots almost into alignment with the $1\bar{1}2$ spots. This orientation relationship is close to the one first reported by Burgers[1], and is summarized in a composite stereogram in Fig. 1(b).

(b) Morphology

The morphology of the carbide precipitates was deduced from a number of micrographs such as Fig. 2(a). Two typical precipitates are shown in the correct orientation to the diffraction patterns displayed below. The foil orientation was {100}, and elongated precipitates were found either along <110> directions with the long interface edge-on (left) or along <100> directions with the long interface inclined at 45° to the foil surface (right). An analysis of the diffraction patterns showed that the first type of precipitates was viewed along the [001] direction and the second type along [100] or [010] in the notation of the stereogram in Fig. 1(b). It was concluded that the observed morphology was only consistent with plate shaped carbide precipitates lying on (110) planes of the tantalum metal matrix. This point is illustrated in Fig. 2(b) where two different {100} sections, corresponding to the thin foil sections in Fig. 2(a), are shown in relation to the bulk crystal. Obviously only a thin plate shaped precipitate will lead to the observed structure of elongated particles with vertical or inclined interfaces. It is clear from the schematic that the long interfaces of the precipitates are in fact the same broad interface viewed from different angles. Frequently a more complex morphology was observed which was invariably due to the coalescence of plates lying on different {110} planes of the matrix. An example is shown in Fig. 3 where the foil normal was again <100>. The same two variants as in Fig. 2(a) are present in the spot pattern and the two parts of the composite precipitate show inclined and vertical interfaces with the matrix. The boundary between the two variants is straight and lies along a <100> direction of the matrix, clearly a special boundary in the carbide system. Careful analysis showed this boundary to be close to a $(1\bar{1}02)$ twin boundary

of the carbide. $(1\bar{1}01)$ twins were also found and it was concluded that particle coalescence must lower the total interface energy by replacing two non-coherent interphase boundaries with one, ideally coherent, twin boundary in the carbide.

(c) Interface Structure

Having established the morphology of the carbide particles, an analysis of the interphase boundaries could best be performed on single plates of Ta_2C {100} foils. Fig. 4 shows a high angle tilt experiment on such a sample. The surface orientation was (010) (Fig. 4(b)). In this orientation, the long interfaces were inclined 45° to the beam while the ledge at A appeared edge-on, following the (101) close-packed planes of the matrix. After a 45° tilt to a $(\bar{1}10)$ zone, the long faces were seen edge-on (Fig. 4(a)). In this position the interface plane could be determined directly, independent of the foil surface. The $[001]$ trace shows that in the thin part of the particle above the ledge, the boundary deviated slightly from the exact (110) plane. This deviation was accommodated by a set of lattice dislocations which were clearly visible when the interface was viewed face-on (see arrow in Fig. 4(c)). The lower part of the interface, closely following (110) planes appeared to be essentially free of lattice dislocations. Fig. 5 shows a typical $\underset{\sim}{g}.\underset{\sim}{b}$ contrast analysis of an interface deviating from the close-packed (110)/(0001) planes. In Fig. 5a) and b) two sets of dislocations are visible. The mixed dislocations in a), spaced about 40 nm apart are out of contrast in b), and the dislocations in b) with a regular spacing of about 15 nm are out of contrast in a). The same dislocations showed only weak residual contrast when imaged under similar conditions with the carbide crystal in diffracting condition (compare the parallel g-vectors of Figs. 5(a) and (d) and 5(b) and (c)).

Both sets of dislocations are also invisible in Fig. 5(e) where a different g-vector of the particle was excited. This analysis led to the conclusion that deviations from the ideal interface boundary on (110)/(0001) planes were accommodated by dislocations with Burgers vector a/2 <111> on the matrix side of the interface.

Fig. 6 shows a lattice fringe image of an ideal (110)/(0001) boundary viewed edge-on in a $(00\bar{1})$ orientation. Note the doubling of the fringe periodicity in the precipitate (P) which is due to carbon ordering. The interface is marked by arrows which indicate that it is exactly parallel to the close packed planes. Another interface is seen in the two high resolution images in Fig. 7. Again, it is viewed edge-on, but it was not a straight boundary. The orientation here was $(1\bar{1}\bar{1})$. At low magnification it appeared to be curved at an angle to the close packed planes. That this curvature was made up of segments along close packed {110} planes is clearly visible in the lattice fringe images of (110)/(0001) and (101) planes in Fig. 7 left and right. In the short segments following the (101) planes (see A and B), the (110)/(0001) planes made a 60° angle with the interface. Thus the mismatch between these two sets of planes had to be accommodated in these short segments. Burgers circuits drawn around these segments in the left part of Fig. 7 indeed show closure failures of one and two (110) planes at B and A. This proves that dislocations are present in curved interfaces and, in agreement with the analysis of Figs. 4 and 5, the contrast in Fig. 7 is consistent with a/2 $[11\bar{1}]$ dislocations.

The short interface making up the perimeter of the precipitate plates was analysed in a similar manner. The carbide in Fig. 8 shows an array of straight dislocation lines with a typical spacing of about 5 nm. These dislocations were again analysed as matrix dislocation with a Burgers vector of

a/2<111>. Fig. 9 shows an example of the structure of the short interface with the same line spacing of about 5 nm at high resolution. The superlattice fringe spacing in the precipitate (P) was d_{0001} = 0.495 nm while the matrix spacing was d_{110} = 0.234 nm ($2d_{110}$ = 0.467 nm). The mismatch of 5.8% can be completely accommodated by an array of matrix dislocations with Burgers vector $a/2[111]$ spaced 18 (110) planes apart. This was exactly the spacing of the optically dense areas in Fig. 9, as indicated by arrows on every 18th plane. This observation suggests that the carbide plates were enveloped by large dislocation loops around their perimeter stacked with a spacing of 18 {110} planes. These loops would be of vacancy type since they have to accommodate an expansion in the precipiate. Using the terminology recently suggested by Olson and Cohen[2] the loops, part of which are seen in Fig. 9, are anticoherency dislocations. Thus the precipitate is regarded as originally coherent in this interface (note lattice fringe continuity across the boundary). Increasing coherency stresses caused by the thickening of the platelet can be related to a set of fictitious "coherency dislocations"[2] which react with a set of real anticoherency dislocations to relieve the long range coherency stresses. This mechanism is in accord with the observation of strings of interstitial loops punched out in the early stages of precipitate growth. These interstitial loops, would leave behind an equal number of vacancy loops at the precipitate. A similar mechanism is difficult to visualize for the broad (110)/(0001) interface because the distortions necessary to maintain coherency across this boundary are more complicated than the simple expansion that dominates the short interface. The pure deformation combined with the 5^{o} rigid body rotation visible in the (110)/(0001) pattern in Fig. 1(a) leads to an effective total

deformation of combined shear and expansion.[3] To compensate such a coherency distortion by anticoherency dislocations would require a closely spaced dislocation network. No such network was found in the ideal boundary on either the matrix or the precipitate side. Hence it was concluded that this boundary must contain a network of mismatch dislocations which are part of the boundary structure analogous to intrinsic dislocations in grain boundaries. Obviously, the resulting interface structure is one of low energy since the precipitate plates were always found to be on this habit plane.

In summary, the morphology of Ta_2C carbide precipitates in tantalum was one of plates on the {110} planes of the matrix. Globular precipitates which were also found were always due to the coalescence of several precipitate variants usually separated by special low energy boundaries. The (0001) basal plane of the precipitate was nearly parallel to the (110) plane of the matrix. The broad interface closely followed these two planes which had a 5.8% mismatch in spacing. Any deviations from this ideal interface plane were made up of microscopic facets on other close packed planes. These facets contained a/2 <111> lattice dislocations on the matrix side of the interface accommodating the 5.8% difference in spacing between matrix and precipitate planes. The same mechanism was found to apply to the short interface making up the perimeter of the platelike precipitates.

ACKNOWLEDGEMENTS

Financial support was provided by the Division of Materials Science, Office of Basic Energy Sciences, U.S. Department of Energy under Contract No. W-7405-Eng-48.

REFERENCES

1) W. G. Burgers, Physica 1, 561 (1934).

2) G. B. Olson, M. Cohen, Acta Met. 27, 1907 (1979).

3) U. Dahmen, K. H. Westmacott, G. Thomas, submitted to Acta Met.

FIGURE CAPTIONS

Fig. 1(a) Selected area diffraction patterns of hexagonal Ta_2C carbides in a cubic Ta matrix showing the relative orientation of the two lattices.

Fig. 1(b) Stereographic projection of the orientation relationship determined from spot patterns as in Fig. 1(a).

Fig. 2(a) Two typical carbide precipitates in a {100} foil with corresponding diffraction patterns. The arrows point to an inclined interface.

Fig. 2(b) Schematic of {110} carbide plates in a cubic matrix with (100) and (001) thin sections corresponding to Fig. 2(a).

Fig. 3 Carbide particle made up of two variants separated by low energy boundary. The diffraction pattern shows them to be nearly twin oriented.

Fig. 4 90^{o} tilt experiment showing (110) interface edge-on in a) and face-on in c). Note ledge on (101) at A and interface dislocations in c) (arrow).

Fig. 5 Contrast experiment on dislocations in an interface deviating from (110)/(0001) plane.

Fig. 6 Lattice fringe image of ideal straight (110)/(0001) interface (see arrows). Doubling of the fringe spacing on the left is due to carbon ordering in Ta_2C.

Fig. 7 Lattice fringe images of curved interface showing ledges along close packed planes and location of mismatch.

Fig. 8 Array of straight matrix dislocations in the short interface.

Fig. 9 Inclined short interface in a lattice fringe image. Arrows on every 18th plane indicate dislocation spacing necessary to completely accommodate mismatch.

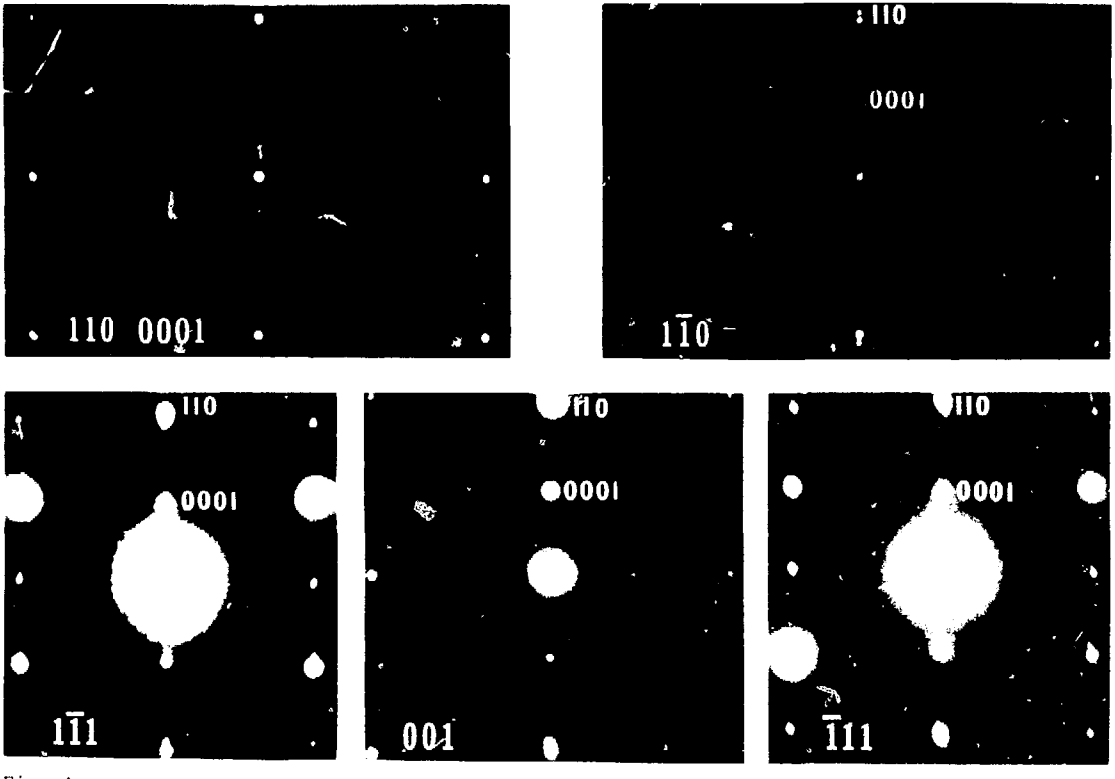

Fig. 1a

XBB799-11718

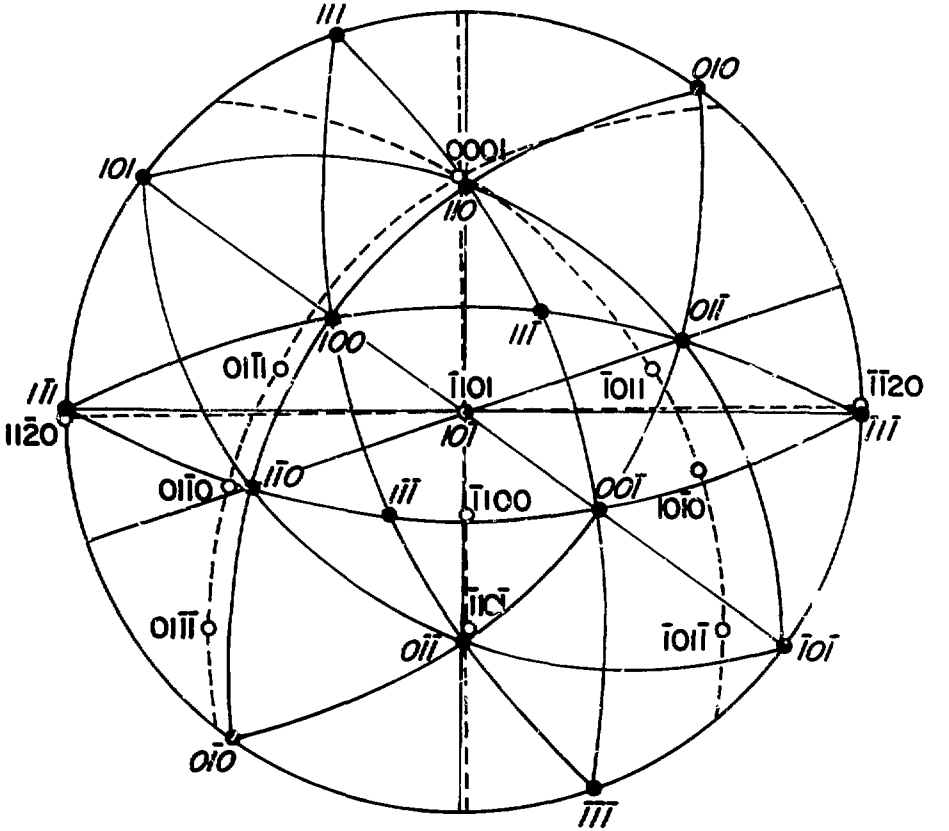

Fig. 1b

XBL7812-6259

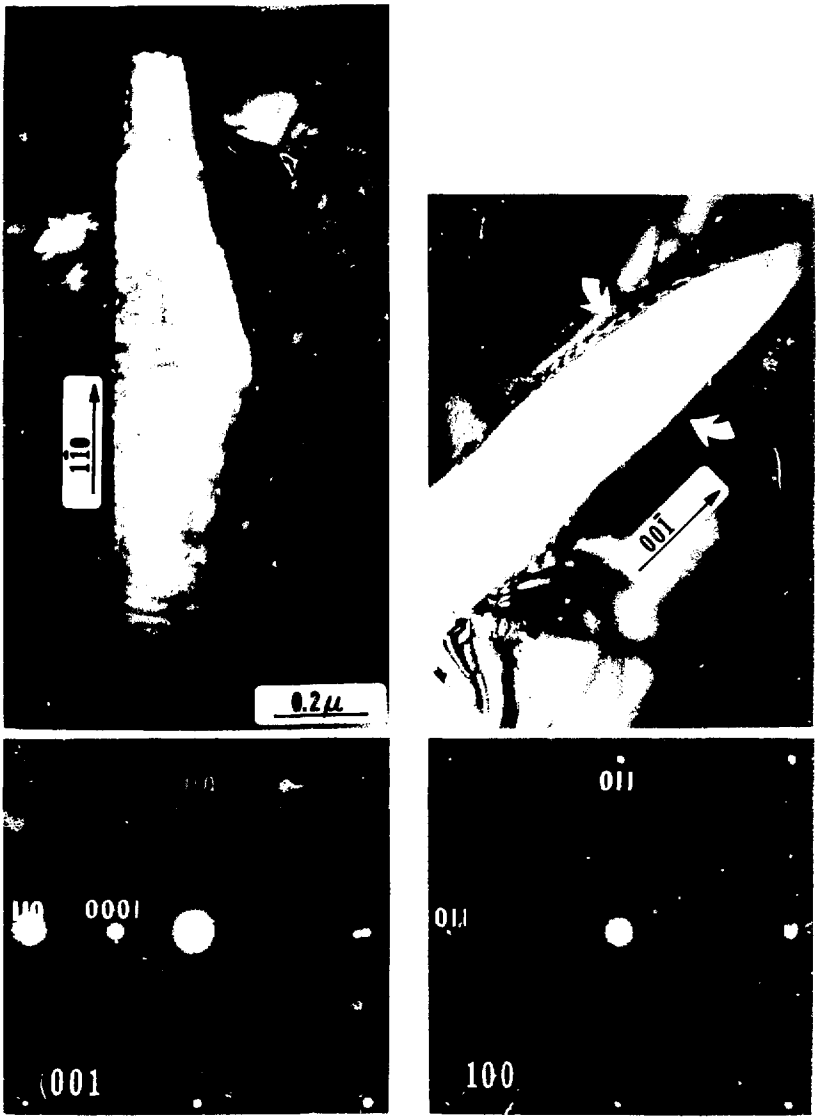

Fig. 2a

XBB799-11717

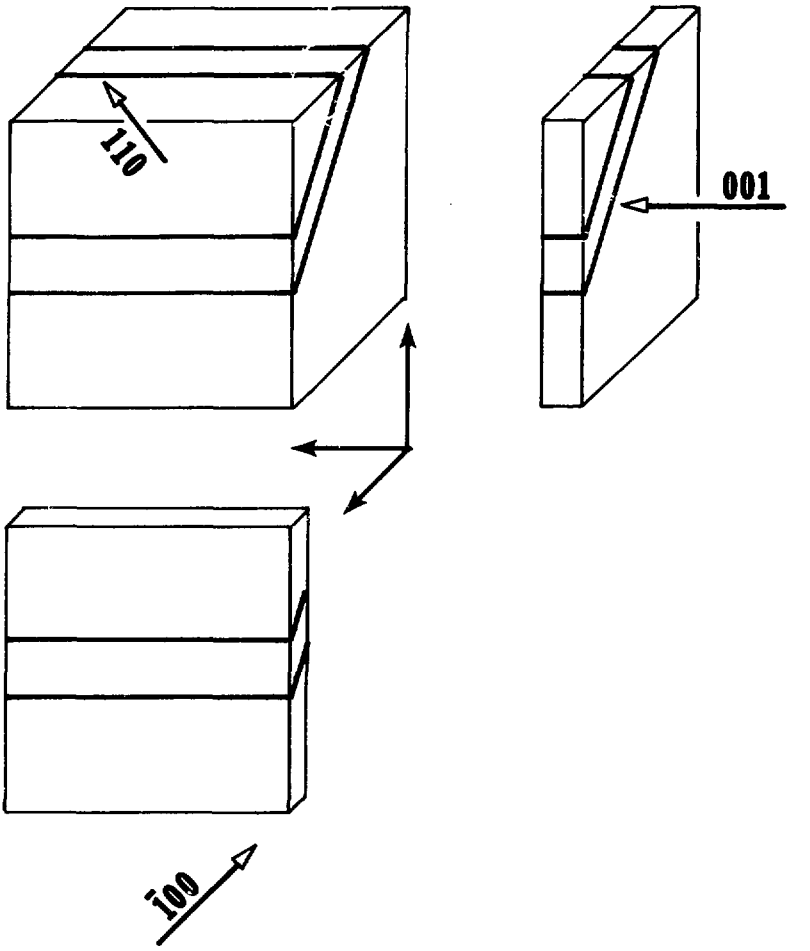

Fig. 2b

XBL 799-11717

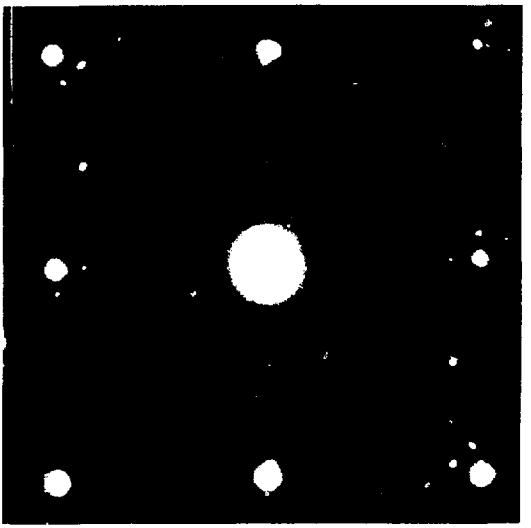

Fig. 3

XBB799-11716

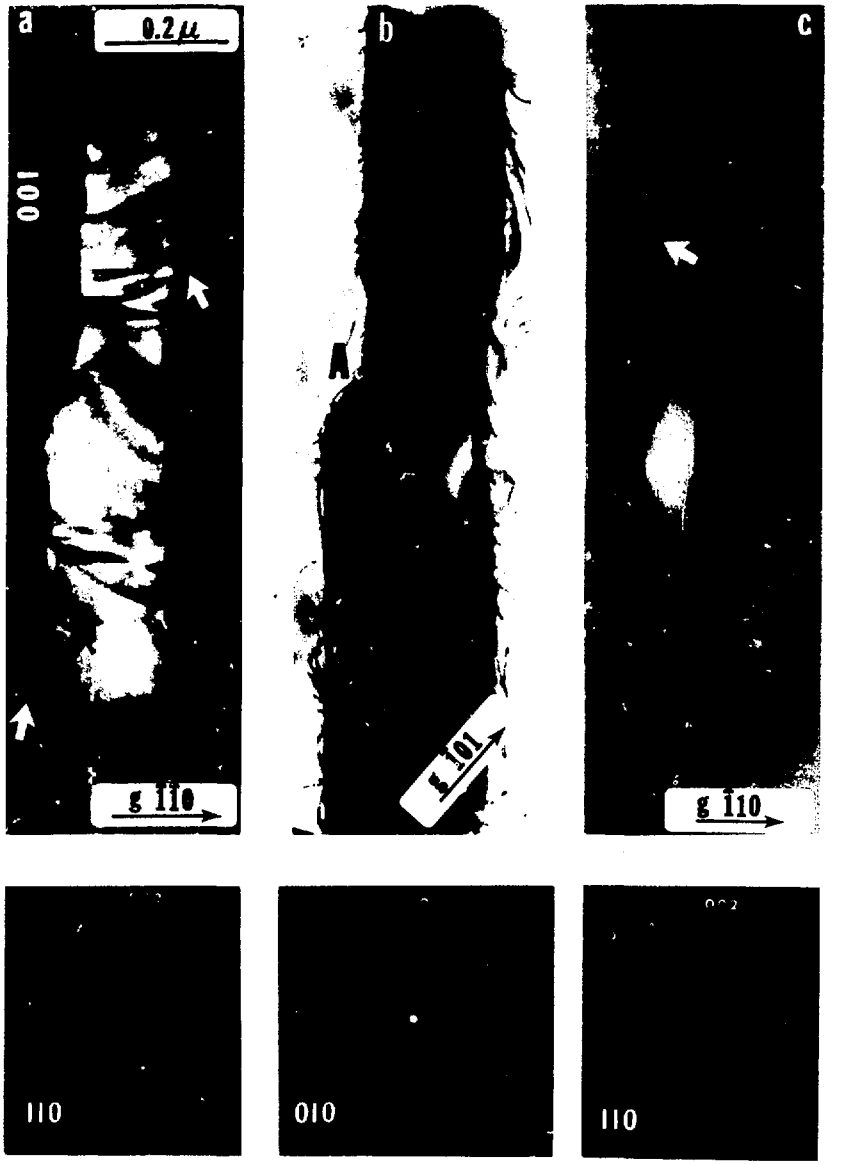

Fig. 4

XBB799-11719

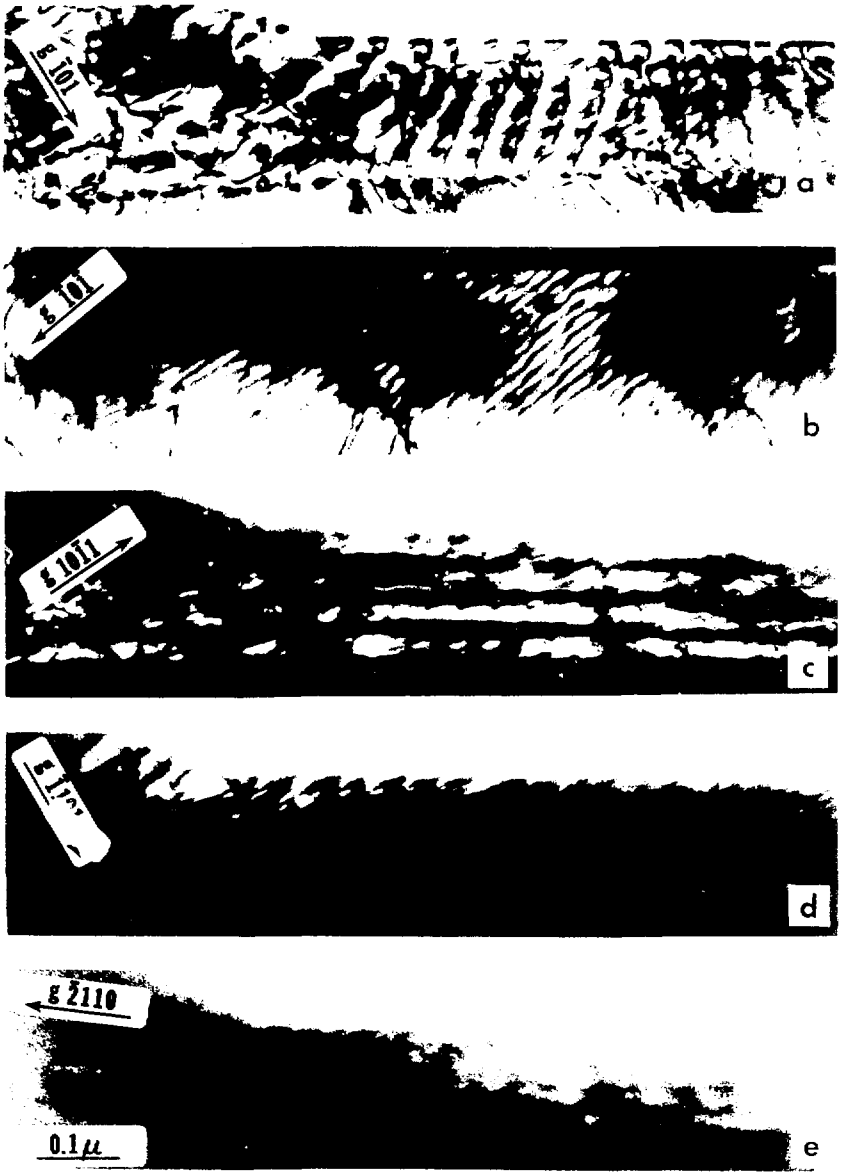

Fig. 5

XBB790-14886

Fig. 6

XBB780-15654

Fig. 7

XBB789-12293

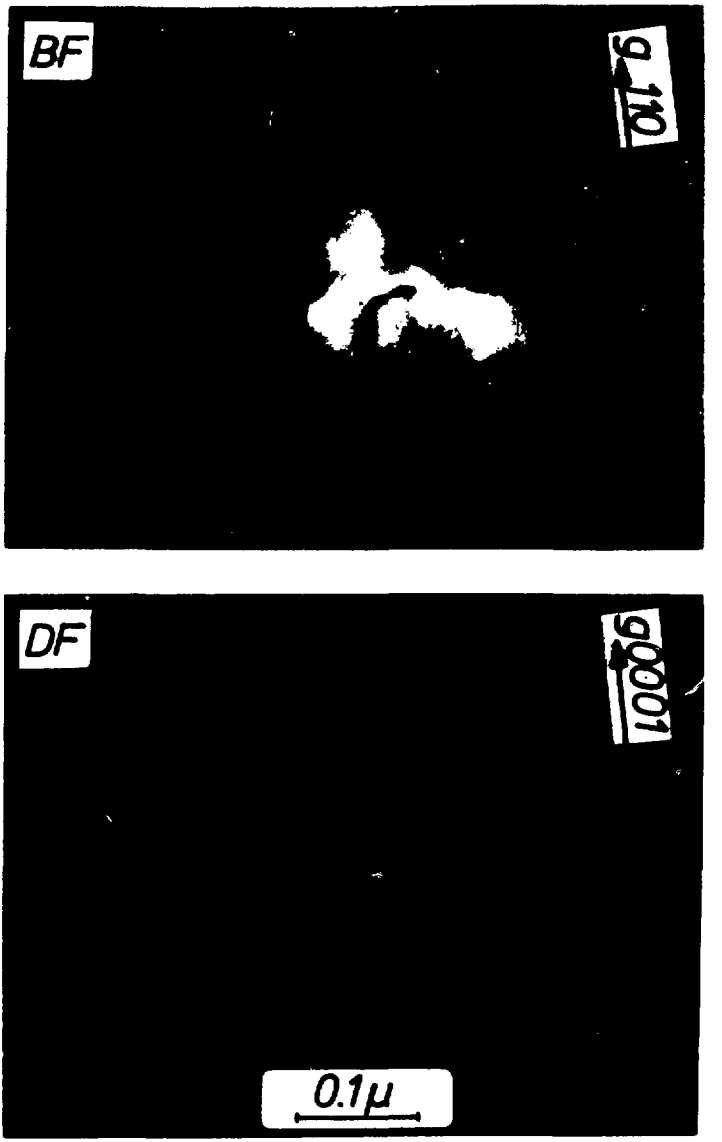

Fig. 8

XBB780-15045

Fig. 9

XBB780-15656